Journal of Applied Polymer Science

Modification of Theoretical Models to Predict Mechanical Behavior of PVC/NBR/Organoclay Nanocomposites

E. Esmizadeh, G. Naderi, Mir Hamid Reza Ghoreishy
Iran polymer and Petrochemical Institute, P.O. Box: 14965-115, Tehran, Iran
Correspondence to: G. Naderi (E-mail: G.Naderi@ippi.ac.ir)

ABSTRACT: Organo-modified nanoclay (Cloisite 30B) was added via direct melt mixing to the acrylonitrile butadiene rubber/poly(vinyl chloride) (PVC/NBR) to fabricate polymer blend/clay nanocomposites. The states of nano-fillers dispersion were investigated by transmission electron microscopy (TEM) and X-ray diffraction (XRD). From the morphological study of nanocomposites, it is concluded that exfoliated morphology is obtainable by introduction of 2.5 vol % of nanoclay. The effect of nano-filler volume content on the mechanical properties of PVC/NBR matrix reinforced by Cloisite 30B was investigated by tensile test. Experimental results show that the Young's modulus and tensile strength of composites can significantly improved with a small amount of nanofiller. Moreover, to investigate the stress–strain behavior of NBR/PVC nanocomposites, seven constitutive models such as Arruda–Boyce, Mooney–Rivilen, Marlow, second order of polynomial, Van der Waals, and third order Odgen were studied and compared with experimental data. Results showed that Malow and second order polynomial model can be used for nanoclay-filled compound whereas the other models show more deviation from experimental data. Three micromechanical models named liner rule of mixtures (LROM) and the inverse rule of mixtures (IROM). Halpin–Tsai theory was applied to evaluate the dependence of Young modulus of nanocomposites on volume fraction of nanofiller. Two modifying factors were proposed to evaluate the Young's modulus of nanocomposites which could greatly improve the theoretical prediction obtained from inverse rule of mixtures (IROM) and Halpin–Tsai equation. The modifying factors were introduced by adopting an exponential, power-law and linear factors in the equation. In order to verify the suitability of the modified models, the ensuing theoretical predictions are compared to the other experimental data available in the literature. Good predictability of the modified models is demonstrated in the results. © 2013 Wiley Periodicals, Inc. J. Appl. Polym. Sci. 000: 000–000, 2013

KEYWORDS: clay; mechanical properties; poly(vinyl chloride)

Received 15 February 2013; accepted 15 May 2013; Published online 00 Month 2013
DOI: 10.1002/app.39556

INTRODUCTION

In recent years, thermoplastic elastomers (TPEs) and thermoplastic vulcanizates (TPVs) blends of acrylonitrile–butadiene rubber (NBR) and poly(vinyl chloride) (PVC) have become technologically have been widely used in industrial applications such as wires and cable coatings, conveyor belt covers, warping films for the food industry, cable jackets, hose cover linings, gaskets, footwear, and cellular products.[1,2]

One approach to improve the final performance of polymer blends is by means of reinforcing nanofillers such as nano-clays and carbon nano-tubes. The recent theoretical and experimental investigations indicate that they have properties suitable for applications in the field of polymer.[3,4] Many researches on carbon nano-tube/polymer composites reported considerable increases in mechanical properties with addition of CNTs at very low volume.[5] Besides, nanoclay or layered silicates, as a natural product, have attracted much attention recently, because of their outstanding mechanical properties (tension young modulus about 170 GPa), large surface area and ion-exchange capacity.[6]

During the last decade, there are many research articles and several reviews that present theoretical models to predict mechanical properties of nanofillers-reinforced polymer composites. Several specific micromechanical techniques models were proposed to evaluate the dependence of mechanical properties of polymer based composites on the volume fraction of the reinforcement,[7] including rule of mixture, Guth model,[8,9], Mori–Tanaka model,[10,11] Halpin–Tsai model,[12,13] Tandon-Weng,[14] rule of mixture,[15,16] and Halpin-kardos model.[17] Orientation,[18] dispersion statue,[19,20] buckling,[21] volume fraction,[21] aspect ratio, and type of nanofillers[22,23] plays an important role in determining the effective properties of polymer nanocomposites. An excellent survey of the research work for predicting the

mechanical behavior of polymer composites has been published by Termonia et al.[24] that introduced a numerical finite-difference model to study the factors controlling the nanocomposite modulus for the case of nano-platelets and nano-tubes. In another study, Rafiee et al.[25] claimed the observed superiority of graphene platelets over carbon nanotubes in terms of mechanical properties enhancement may be related to their two-dimensional (planar) geometry. Various dispersion methods (e.g., stirring, extrusion, kneading, sonication, etc.) have been applied to distribute nanofillers in polymer matrix.[26] In this study, internal mixer brabender (shear mixing) technique was used to exfoliates agglomerates and disperses nano-fillers in the matrix effectively.

TPEs and TPVs present a very complicated mechanical behavior that exceed linear elastic theory and contain large deformations, plastic and viscoelastic properties.[27] Due to the deviation of their behavior from the linear elastic state, some investigators have studied the use of hyperelastic models for these compounds.[28,29] For example, stress–strain behavior of NR/EPDM composite reinforced with nanoclay was presented by Alipour et al.[28] They employed five hyperelastic models including second order Polynominal, Yeoh, third order Ogden, Marlow, and Arruda–Boyce to find a relationship between the nanoclay content and degree of fitting of hyperelastic models for nanocomposites.[28]

According to our comprehensive survey of the literature, no study has been published on the stress–strain behavior of PVC/NBR nanocomposites using hyperelastic models. So, the effect of nanoclay loading on the applicability of five material models including Mooney—Rivilen, second order Polynominal, third order Ogden, Marlow, and Arruda–Boyce is investigated. The purpose of this article is to better understand the origin of the superior reinforcing efficiency observed in well-exfoliated polymer-based nanocomposites compared to conventional composites using composite theory including liner rule of mixtures (LROM) and the inverse rule of mixtures (IROM). Halpin–Tsai theory was applied to evaluate the effects of filler geometry, and orientation on the young modulus of PVC/NBR nanocomposites. A modified form of Halpin–Tsai theory and inverse rule of mixtures (IROM) equations including an exponential shape factor, aspect ratio of filler, orientation factor, power-law parameter, and linear factor are proposed to accurately predict the mechanical properties of PVC/NBR nanocomposites, for nanoclay filled polymer matrix. Model predictions are compared to experimental morphological and mechanical property data for nanoclay nanocomposites based on PVC/NBR. Moreover, we have tried to find a relationship between nanofiller loading and degree of fitting for the mechanical data of nanocomposites available in the literature.

THEORETICAL CONCEPT

Halpin–Tsai Theory

According to literature, Halpin–Tsai and the modified Halpin–Tsai equation is widely applied to describe the young moduli of compound filled with various types of filler.[3,5,6,13,21] It should be noted that Halpin–Tsai equation predicts the dependence of young modulus of reinforced-composite between two bounds as follows. The upper and the lower bounds are given by the liner rule of mixtures (LROM) and the inverse rule of mixtures (IROM) as eqs. (1) and (2), respectively[30]:

$$E_{c(\mathrm{LROM})} = E_f \varphi_f + E_m(1-\varphi_f) \tag{1}$$

$$E_{c(\mathrm{IROM})} = \left(\frac{\varphi_f}{E_f} + \frac{(1-\varphi_f)}{E_m}\right)^{-1} \tag{2}$$

where E_c, E_f, and E_m are longitudinal elastic modulus of composite, filler, and matrix, respectively, and φ_f is the volume fraction of the reinforcing filler. According to Halpin–Tsai equation, the engineering modulus for fully aligned-composites is expressed in eq. (3):

$$E_{c(\mathrm{Halpin-Tsai})} = E_m\left(\frac{1+\lambda\eta\varphi_f}{1-\eta\varphi_f}\right) \tag{3}$$

in which $\eta = \frac{E_f/E_m - 1}{E_f/E_m + \lambda}$. λ is a shape factor depending upon filler orientation, geometry, aspect ratio, and loading direction.[11] It is important to note that the composite Young's modulus is composed of two components, parallel modulus (longitudinal), and perpendicular (transverse) to the major axis of the fillers. Therefore, for randomly oriented the expression is rather sophisticated[3]:

$$\frac{E_c}{E_m} = a_L\frac{1+\lambda_L\eta_L\varphi_f}{1-\eta_L\varphi_f} + a_T\frac{1+\lambda_T\eta_T\varphi_f}{1-\eta_T\varphi_f} \tag{4}$$

where a_L, a_T, λ_L, and λ_T take the value of $^3/_8$ and $^5/_8$, $2^l/_d$ and 2, respectively.

Hyperelastic Models

The stress–strain behavior of hyperelastic materials can be explained as the strain energy density (SED) stored in the material based on three invariants of the strain tensor (I_1, I_2, I_3) as[29,31,32]:

$$U = f(I_1, I_2, I_3) \tag{5}$$

where U (or W) is strain energy density and I_1, I_2, and I_3 are three invariant of deformation tensor given by:

$$\begin{cases} I_1 = \lambda_1^2+\lambda_2^2+\lambda_3^2 \\ I_2 = \lambda_1^2\lambda_2^2+\lambda_2^2\lambda_3^2+\lambda_3^2\lambda_1^2 \\ I_2 = \lambda_1^2\lambda_2^2\lambda_3^2 \end{cases} \tag{6}$$

in which λ_1, λ_2, and λ_3 are the three principal stretch ratio. Equation (6) can be given as:

$$U = \sum_{i+j+k=1}^{\infty} C_{ijk}(I_1-3)^i \cdot (I_2-3)^j \cdot (I_3-1)^k \tag{7}$$

A simple extension is defined by $\lambda_1=\lambda$, $\lambda_2=\lambda_3=\lambda^{-1/2}$. Where $I_3=0$ for a perfect incompressible material that volume remains unchanged on deformation, therefore eq. (7) decreases to:

$$U = \sum_{i+j=1}^{\infty} C_{ij}(I_1-3)^i \cdot (I_2-3)^j \tag{8}$$

In this research, some material models used for prediction of non-linear elastic behavior of Virgin PVC/NBR and PVC/NBR

Table I. Code and Formulation of PVC/NBR Nanocomposites

Material	PN = Reference	PNC-1.5	PNC-2.5	PNC-3.5
Cloisite 30B (vol %)	0	1.5	2.5	3.5
ZnO	5	5	5	5
Stearic acid	1.5	1.5	1.5	1.5
MBTS	1	1	1	1
TMTD	0.5	0.5	0.5	0.5
Sulfur	2	2	2	2

P = PVC, N = NBR, C = Cloisite 30B

nanocomposites. The application, corresponding variables, and the available data to determine material parameters of the model identifies what kind of hyperelastic model should to be used. In this study, seven hyperelastic material models have boon investigated to depict nonlinear stress–strain behavior of PVC/NBR nanocomposite samples. It should be noted that the full incompressibility assumption is applied for all models, meaning that all the equations only contain the deviatoric part and the volumetric part is neglected.

Arruda–Boyce. This model represents the underlying molecular structure of the rubbers to simulate the non-Gaussian behavior of individual chains in the network.[29,33] The form of the Arruda–Boyce strain energy potential for incompressible material is assumed to be equal to the sum of individual chains oriented in space randomly[34]:

$$U = \mu \sum_{i=1}^{5} \frac{C_i}{\lambda_m^{2i-2}} \left(I_1^i - 3^i\right) \tag{9}$$

In the above equation, C_i s are material constants where $C_1 = \frac{1}{2}$, $C_2 = \frac{1}{20}$, $C_3 = \frac{11}{1050}$, $C_4 = \frac{19}{7000}$, and $C_5 = \frac{519}{673750}$. The quantity

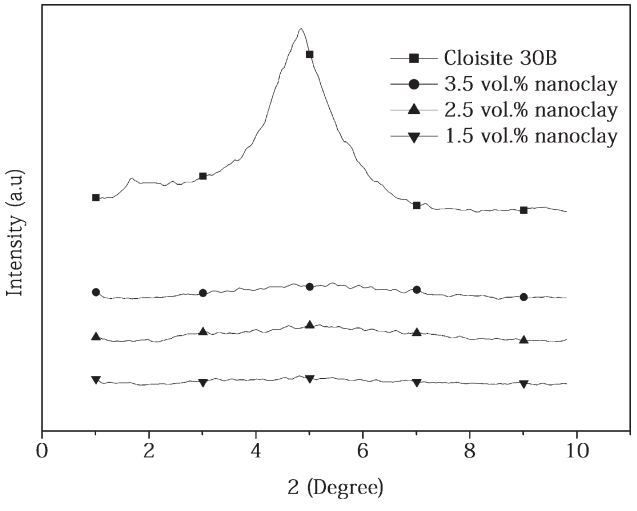

Figure 1. X-ray diffraction profiles for Cloisite 30B and PVC/NBR/nanoclay.

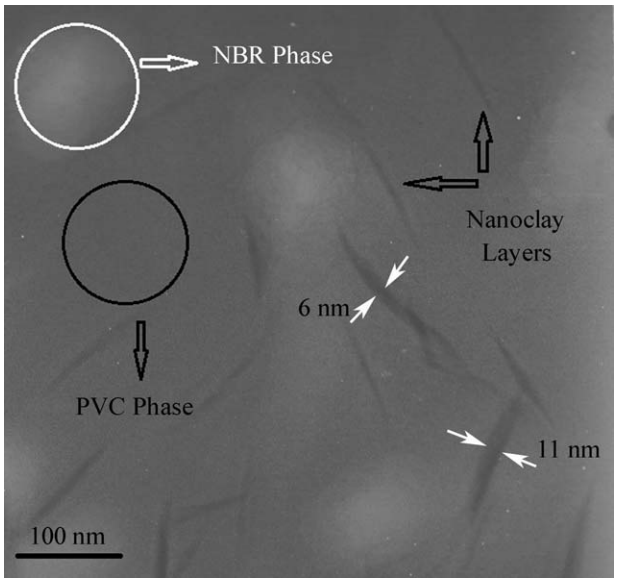

Figure 2. TEM micrograph of PVC/NBR nanocomposite sample with 3.5 vol % of nanoclay.

μ is initial shear modulus and λ_m can be interpreted as a measure of the limiting network stretch or locking stretch, at which upturn of stress–strain curve rises significantly.

Strain energy function is dependent of the first invariant of the left deviatoric Cauchy–Green tensor, neglecting any influence from the second stretch invariant for Arruda–Boyce model. With neglecting second invariant of left Cauchy–Green tensor, Arruda–Boyce model, helps to make accurate solution in the range of smaller strains. A sufficient accuracy in both small and large strain is obtainable using higher values for locking stretch parameter.[35]

Polynomial. The principal structure of this model expressed based on 1st and 2nd invariant $\overline{I_1}$ and $\overline{I_2}$ of deviatoric Cauchy–Green tensor as below:

$$U = \sum_{+j=1}^{\infty} C_{ij} \left(\overline{I_1} - 3\right)^i \cdot \left(\overline{I_2} - 3\right)^j \tag{10}$$

in the above equation C_{ij} is material constant describes shear behavior of material, while N is a positive determining number of terms in strain energy function (N = 1,2,3). This model has usually been chosen to describe the strain–stress behavior of filled elastomers, with 4–5 terms.[27]

Table II. Mean Values of Mechanical Properties of PVC/NBR Nanocomposites Compared to the Pure Matrix

Sample	Tensile strength	Modulus	Elongation at break
Reference	12.68	3.4	160
PNC-1.5	19.1	3.8	142
PNC-2.5	25.2	5.4	111
PNC-3.5	28.1	6.3	87

Applied Polymer SCIENCE

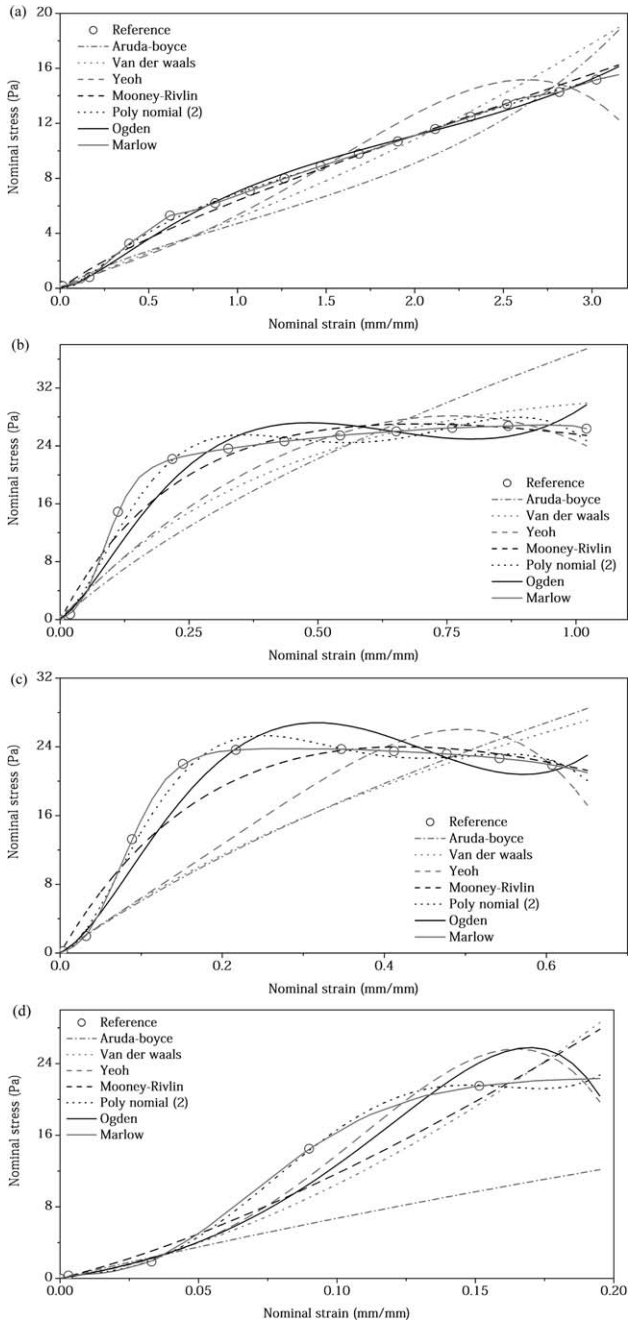

Figure 3. Nominal stress versus nominal strain for nanoclay-filled sample; (a) Reference, (b) PNC-1.5, (c) PNC-2.5, and (d) PNC-3.5.

Van der Waals. The strain energy potential in Van der Waals model is

$$U=\mu\left\{-(\lambda_m^2-3)[\ln(1-\eta)+\eta]-\frac{2}{3}a\left(\frac{\tilde{I}-3}{2}\right)^{\frac{3}{2}}\right\} \tag{11}$$

where $\tilde{I}=(1-\beta)\overline{I_1}+\beta\overline{I_2}$ and $\eta=\sqrt{\frac{\tilde{I}-3}{\lambda_m^2-3}}$

here μ is the initial shear modulus; λ_m is the locking stretch; a is the global interaction parameter; β is an invariant mixture parameter. The Van Der Waals model is also known az the Killian model [36].

Ogden. Ogden proposed the strain density function can be described directly based on principal stretch ratios for incompressible materials. Ogden strain density can be given as follows:

$$U=\sum_{i=1}^{N}\frac{2\ \mu_i}{\alpha_i^2}(\overline{\lambda_1}^{\alpha_i}+\overline{\lambda_2}^{\alpha_i}+\overline{\lambda_3}^{\alpha_i}-3) \tag{12}$$

where $\overline{\lambda_i}=J^{-\frac{1}{3}}\lambda_i$, $J=\lambda_1\lambda_2\lambda_3$. J is Jacobian determinant, μ_i and α_i are material constants which describe shear. In this study, it is assumed that $N=3$. Calculation of invariant derivatives of Ogden energy function is more complicated than that of polynomial form. Therefore, Ogden model is more accurate in fitting, when data are available from multiple experimental tests.[37]

Mooney–Rivlin. Mooney–Rivlin's strain energy potential is introduced as:

$$U=\sum_{i,j=0}^{N}C_{ij}(\overline{I_1}-3)^i\cdot(\overline{I_2}-3)^j \tag{13}$$

where C_{ij} is material constant describes shear behavior of material and $C_{00}=0$. By assuming $N=2$, $\alpha_1=2$ in Ogden model or $N=1$ in polynomial model, the specific type of Mooney–Rivlin model is given as:

$$U=C_{10}(\overline{I_1}-3)+C_{01}(\overline{I_2}-3) \tag{14}$$

Yeoh. This model is a special form of reduced polynomial model. Reduced polynomial model is a simple form of polynomial model by just omitting 2nd invariant of left Cauchy–Green tensor where j is always zero. Thus, strain energy function becomes

$$U=\sum_{i=1}^{N}C_{i0}(\overline{I_1}-3)^i \tag{15}$$

The Yeoh model is a form of reduced polynomial model in which $m=3$ and introduced as:

$$U=\sum_{i=1}^{3}C_{i0}(\overline{I_1}-3)^i \tag{16}$$

This model is offered for describing hyperelastic behavior of rubber compounds for two main reasons as follows:

a. It is able to make accurate solution for a much wider range of deformation
b. It is applicable for prediction stress–strain behavior in different deformation modes while data gained in one simple deformation such as uniaxial extension.[38]

Marlow. There is not any explicit relation between strain energy density and/or invariants or stretch ratios for Marlow model. Thus, it is assumed that the strain energy density is only a function of the first invariant of the strain tensor, so can be written as:

$$U=U(\overline{I_1}) \tag{17}$$

Table III. Statistical Analysis of the Models

	Arruda-Boyce		Van der Waals		Yeoh		Mooney-Rivlin		Polynomial		Ogden		Marlow	
Sample\Model	σ	S_e	σ	S_e	σ	S_e	σ	S_e	σ	S_e	σ	S_e	σ	S_e
Reference	2.01	0.76	1.79	0.67	1.71	0.64	0.55	0.2	0.22	0.08	0.5	0.19	0.33	0.12
PNC-1.5	7.75	3.46	4.47	1.99	3.82	1.71	1.5	0.67	1.03	0.46	2.13	0.95	0.05	0.02
PNC-2.5	7.59	2.87	7.39	2.79	6.26	2.36	2.15	0.81	0.79	0.3	2.20	0.83	0.28	0.1
PNC-3.5	6.86	3.06	4.07	1.82	1.94	0.86	3.25	1.45	0.56	0.25	2.59	1.15	0.47	0.21

σ = standard deviation
S_e = standard error

Since for incompressible material, $I_3=0$, thus I_1 can be shown as below:

$$I_1=\lambda_1^2+\lambda_2^2+\frac{1}{\lambda_1^2\lambda_2^2} \tag{18}$$

It is worth noting that the minimum and maximum values of I_1 is between 3 and $+\infty$, respectively. The uniaxial form of I_1 from eq. (18) ($I_2=1/\sqrt{\lambda_1}$) can be expressed by:

$$I_1=\lambda^2+\frac{2}{\lambda} \tag{19}$$

EXPERIMENTAL

Material

PVC/NBR was selected as polymer matrix due to the miscible nature of PVC/NBR blend as evidenced from single glass transition (T_g) observed in our previous work.[39] Suspension polymerized PVC in powder form, with a *K*-value of 65 was provided by Bandar-e-Imam Petrochemical Company (Iran); NBR (Bound acrylonitrile content = 34%, Mooney viscosity ML (1 + 4) at 100°C = 41) was supplied by Kumho Petrochemical Co. (Korea); Cloisite 30B (CEC 90 mEq/100 g, Young modulus = 170 GPa, aspect ratio = 200) natural montmorillonite modified with a quaternary ammonium salt: (methyl bis-2-hydroxyethyl tallow ammonium) methyl tallow bis-2-hydroxyethyl quaternary ammonium (Southern Clay Products, TX). The vulcanization curatives: stearic acid (SA), Zinc oxide (ZnO), sulphur (S), tetramethyl thiuram disulphide (TMTD), and mercapto benzthiazyl disulphide (MBTS) were of commercial grade.

Preparation of NBR/PVC Nanocomposites

The formulations of the blends are given in Table I. The Brabender internal mixer was applied at 160°C and a rotor speed of 50 rpm in order to disperse Cloisite 30B (with concentration given in Table I) in PVC/NBR (70/30) thermoplastic–elastomer matrix. There are two types of material for investigation. One type of samples used for morphological features do not have curing agent and the other type used for mechanical investigation which possess curing agent. At first PVC and nanoparticle was charged into the mixing chamber and NBR was added after 1 min, then curing agents were added to chamber after 6 min and dynamically vulcanization took place about 1.5 min. The compound was then removed from the mixer and sheeted on a cold two-roll mill. At the end, sheets of 1-mm thickness were prepared by hydraulic press with a pressure of 1.5 MPa at 160°C.

Characterization

A static stress–strain which is commonly used for evaluating effect of various compounding ingredient in rubber industry is applied. Tensile tests were performed on 1 mm thick dumbbells at room temperature using an Instron 8511 machine at a deformation rate of 50 mm/min according to ASTM D-412. The dumb-bell specimens were cut from molded sheets. Five specimens were tested and the mean value was taken for each formulation. In order to characterize the dispersion and the morphology nano-fillers in PVC/NBR matrix, microscopic techniques were applied. Transmission electron microscopy (TEM) analysis was performed with a Philips apparatus using an acceleration voltage of 120 kV. The structure of layered silicates and the morphology of nanoclay/PVC/NBR composites are analyzed by X-ray scattering. X-Ray diffraction (XRD) data are collected on a Philips X'Pert PRO (The Netherlands) with Cu $K\alpha$ radiation of wavelength 1.54 Å using an accelerating voltage of 40 kV. Diffraction spectra are obtained over a 2θ range of 2–10°

Table IV. Material Parameters of Arruda–Boyce and the Third Order Ogden Models for Prepared Samples

Model	Arruda-Boyce			Ogden 3					
Sample	μ	μ_0	λ_m	μ_1	μ_2	μ_3	α_1	α_2	α_3
Reference	2.367	2.546	2.983	82.638	9.102	−81.976	2.277	6.195	−0.470
PNC-1.5	21.067	21.067	2861.744	351.473	33.415	−368.431	−4.611	5.196	−6.871
PNC-2.5	22.180	22.180	1369.906	588.399	26.250	−600.415	−4.296	7.339	−7.262
PNC-3.5	24.266	24.569	6.999	509.729	−171.810	−321.052	18.490	22.286	15.378

Table V. Material Parameters of Yeoh and the Second Order Polynomial Models for Prepared Samples

Model	Yeoh			Polynomial (N = 2)				
Sample	C10	C20	C30	C10	C20	C01	C11	C02
Reference	0.993	0.150	−6.031	13.008	−0.146	−13.326	0.991	−4.813
PNC-1.5	13.096	−1.060	−0.150	251.523	−136.633	−245.362	507.342	−573.176
PNC-2.5	11.373	6.304	−6.267	511.111	−781.529	−509.676	2502.778	−2251.689
PNC-3.5	9.057	375.839	−2114.362	−461.424	86562.973	472.431	−202282.447	118861.180

and the interlayer spacing (d_{001}) is calculated using the Bragg's equation:

$$d_{001} = \frac{\lambda}{2\sin\theta_{\max}} \quad (20)$$

where, λ is the wavelength and d_{001} is interlayer spacing of silicate layers.

RESULTS AND DISCUSSION

Micrography of PVC/NBR Nanocomposite

XRD is a powerful technique to follow the dispersion of organoclay in the polymer matrix and intercalation of polymeric chains into the silicate layers of clay. Figure 1 shows X-ray diffraction patterns of the nanoclay in PVC/NBR nanocomposites. The clay exhibited an apparent peak at $2\theta = 4.8^\circ$ corresponded to $d_{001} = 18.189$ Å. However, there was no peak in the XRD pattern of the PVC/NBR (70/30) nanocomposite. This clearly indicates that polymer chains intercalated into the galleries of the silicate layers and the interlamellar spacing of clay during dry-compounding. The decrease in intensity and the broadening of peaks indicate that the stacks of layered silicates become more exfoliated. Silicate layers of PVC/NBR nanocomposite were not stacked regularly, though an exfoliated morphology is successfully obtained. This can be related to the polar nature of Cloisite 30B which facilitate such interactions between nanoclay and polymer chains as it was shown in our previous works with PVC/NBR (30/70).[39]

Figure 2 shows the TEM images of cryogenically fractured surfaces of PVC/NBR nanocomposite samples in which dark lines represent the Cloisite layers dispersed within the matrix. Light regions depict the phase with lower density (NBR) and darker regions are representatives of the denser phase (PVC); the black lines are related to the cross section of silicate layers.[20,39] The TEM micrograph (Figure 2) implies there is also some small part of nanoclay aggregates through the polymer matrix. The uniform dispersion of nano-fillers in composites reduces the stress concentration and enhances the uniformity of stress distribution; as a result, the nanofiller/PVC/NBR composites are expected to have an improved performance in mechanical properties.

Stress–Strain Behavior of NBR/PVC Nanocomposites by Hyperelastic Models

The ultimate tensile properties reflect the expected trend of behaviors, considering the presence of nano-fillers in PVC/NBR matrix. Table II provides an interesting summary of the mechanical properties of the blends with various amounts of nano-filler.

It is well-known that introduction of a modest amount of nano-filler into a polymer matrix can increase modulus and tensile strength of nanocomposites.[4,8,40] As it can be observed from the Table II, the tensile strength and modulus of the PVC/NBR composite increased approximately two times compared with that of pure PVC/NBR (Reference sample) by introducing 3.5 vol % of nanoclay. This agrees with the data obtained by other researchers with introduction of nano-filler to rubber matrix.[40,41]

In the case of PVC/NBR-clay nanocomposites, this observation can be attributed to the fact that the existence of great interfacial action between the clay layers and the PVC/NBR matrix, which could decrease the expansion energy of the crack. Such improved interaction between polymer matrix and the nanoclay layers could be due to two main reasons. The former is the organo-philic nature of Cloisite 30B with cation exchange capacity of 90 mEq/100 g that granted the needed compatibility via ion exchange process. Alkyl ammonium cations (methyl tallow bis-2-hydroxyethyl quaternary ammonium in the nano-filler implemented in this study) lower the surface energy of natural montmorillonite, thus improve the wetting characteristic of nanoclay with polymer chains. The latter is the high chemical activity of alkyl ammonium cations that can confer some polarity to nanoclay structure. The induced polarity of nanoclay

Table VI. Material Parameters of Mooney–Rivlin and 6th Order Reduced Polynomial Models for Prepared Samples

Model	Mooney–Rivlin		Van der Waals			
Sample	C10	C01	μ	λ_m	α	β
Reference	2.135	−0.623	1.916	790.084	−0.521	0.000
PNC-1.5	−7.790	30.219	27.153	406.068	0.376	0.000
PNC-2.5	−20.724	47.874	23.344	242.528	0.146	0.000
PNC-3.5	105.970	−93.005	16.910	9.875	−10.581	0.000

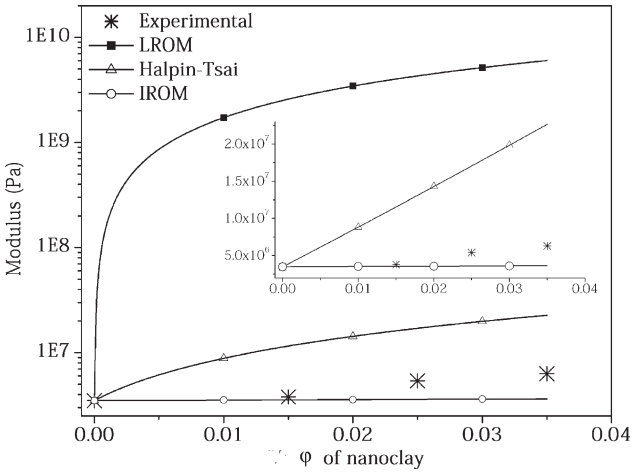

Figure 4. Prediction of Young's modulus of nanoclay-filled PVC/NBR for various values mechanical models.

layers can improve the interface interaction of nanoclay layers and polymeric matrix.[41]

Table II reflects the influence of the nanoclay content on the elongation at break of the PVC/NBR composites. It can be seen that as the two nano-filler level increased the elongation at break showed different trends. It is shown that the elongation at break of the nanoclay-filled prepared formulations continue to drop markedly with the nanoclay level. The downfall of elongation at break with nanoclay content could be attributed to the confinement of polymer chains due to the presence of nanoclay layers, which reduces the mobility of the PVC/NBR chains. Also, the improvement to the state of intercalation/exfoliation of the nanoclay-filled composites can contribute to the decrease in elongation at break.[42] These phenomena will obviously shorten the ability of the matrix to be extended; therefore, short elongation with the clay content was recorded. The decrease of elongation at break in case of (PVC/NBR)–clay nanocomposites were given by some researchers.[41]

Hyperelastic models can be used to predict the stress behavior of elastic composites as a function of applied strain. ABAQUS software uses curve fitting procedures to determine material models by minimization of root mean square or least square fit. In this section, the stress–strain data were imported into ABAQUS software and the behavior of nanocomposites is compared with some hyperelastic models such as: Arruda–Boyce, Mooney–Rivlin, Ogden ($N = 3$), Polynomial ($N = 2$), Reduced polynomial, Marlow Van der Waals, and Yeoh.

To investigate the effect of nanofiller content on the applicability of above-mentioned models, nominal stress versus nominal strain obtained from experimental and model predictions for PVC/NBR nanocomposites with different content of nanofiller is illustrated in Figure 3. The standard deviations and standard error of the fitting models is given in Table III. Material constants obtained from mentioned models are listed in Tables (IV–VI). T4-T6

According to the obtained results for PVC/NBR/Nanoclay nanocomposite samples (Figure 3), it can be pointed that the only Marlow and polynomial models show a good agreement with experimental data in all strain regions. In higher amount of nanoclay which the interaction established between nanoclay layers and polymer chains increases, the deviation of other models becomes more obvious. For example, as the nanoclay content of the samples increases, the theoretical predicted data by Arruda–Boyce and Yeoh models show more disagreement with experimental data in middle and large strains. As nanoclay content of the samples increased, a consequence of the changes of molecular orientation might be such a way that they do not comply with the basic assumption of this model, so the inconsistency between experimental data and model predictions are noticed. So, according to the above results, it can be concluded that the second order Polynomial and Marlow models can truly predict stress–strain behavior of nanocomposite samples in all strain regions with a high degree of accuracy. In nanocomposite samples, the existence of crosslinks changes the behavior of PVC/NBR chains so that the degree of fitting for these models is not satisfactory.

In conclusion, since the material properties are sensitive to changes in manufacturing conditions such as plasticizer content, filler type, filler content, and curing efficiency[27] and these parameters change the dynamic of the macromolecular motions, the necessity of new investigations to evolve new models for depiction of the mechanical treatment of the polymer nanocomposites is become more and more obvious.

A Modified Form of Micromechanical Models

According to the experimental results reported in the literature,[6,7,11,26,43,44] the relationship between mechanical properties of polymer nano-composites and nano-filler loading is not linear. The presented IROM and LROM models by eqs. (1) and (2) are

Table VII. Young's Modulus of PVC/NBR Nanocomposites Predicted by Different Mechanical Models and Proposed Modified Models

		Analytical predictions for different specimens						
Sample	Experimental data	Halpin-Tsai	LROM	IROM	(1) Modified Halpin-Tsai	(1) Modified IROM	(2) Modified Halpin-Tsai	(2) Modified IROM
PNR	3.5e6	3.5e6	3.5e6	3.5e6	3.5e6	3.5e6	3.5e6	3.5e6
PNC1.5	3.8 e6	1.15e7	2.58e9	3.55e6	4.22e6	4.00e6	4.06e6	4.46e6
PNC2.5	5.4 e6	1.70e7	4.30e9	3.58e6	4.79e6	5.06e6	4.88e6	5.25e6
PNC3.5	6.3 e6	2.26e7	6.02e9	3.62e6	6.52e6	6.45e6	6.55e6	6.18e6
Squared error					0.56	0.21	0.33	0.41

Applied Polymer SCIENCE

Table VIII. Parameters for Proposed Modifying Factor of IROM and Halpin–Tsai Models

Sample	Parameters of modifying factor	Nanoclay-filled PVC/NBR
(1) Modified Halpin-Tsai	**a**	6.980
	b	−0.269
	c	9.156
(1) Modified IROM	**a**	47.025
	b	−0.243
	c	19.846
(2) Modified Halpin-Tsai	**a**	0.383
	b	−0.164
	c	−29.829
(2) Modified IROM	**a**	319.047
	b	−0.029
	c	13.537

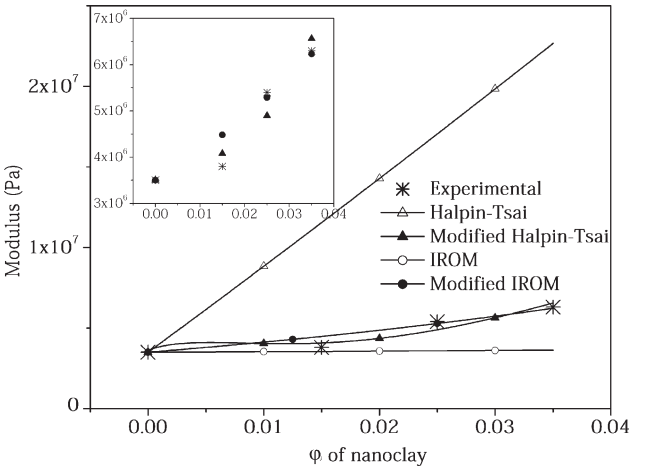

Figure 6. Comparison of the present experimental data and theoretical predicting modified model (II) for the Young's modulus of PVC/NBR nanocomposites.

only able to estimate the Young's modulus of composites with fully (ideally) aligned nanocomposites. Thus, Halpin–Tsai equation (2) was proposed based on introducing an orientation efficiency factor and nano-filler aspect ratio to make an appropriate prediction of the Young's modulus of nanocomposites with randomly oriented nano-filler. Following Table II shows the variation of the mean value of Young's modulus, the tensile strength, and elongation at break of PVC/NBR nanocomposites as a function of nano-filler content in composite. It can be inferred from the figure that the mechanical properties of the composite are significantly improved as the volume fraction of nano-filler is increased. It is also worth pointing out that the maximum values of the Young's modulus are found to be 6.3 MPa, at 3.5 vol % of nanoclay; while the pure PVC/NBR matrix exhibited a Young's modulus of 3.5 MPa. The effect of nano-filler on the composite mechanical properties is very noticeable; for example, only a 3.5 vol % addition of nanoclay can enhance the Young's modulus and the tensile strength of the composite up to 80%.

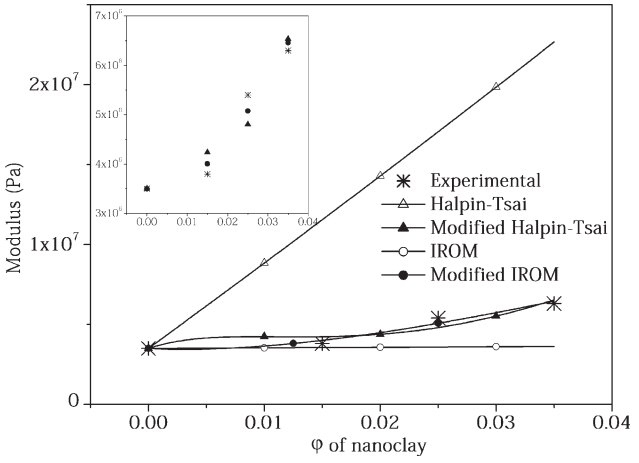

Figure 5. Comparison of the present experimental data and theoretical predicting modified model (I) for the Young's modulus of PVC/NBR nanocomposites.

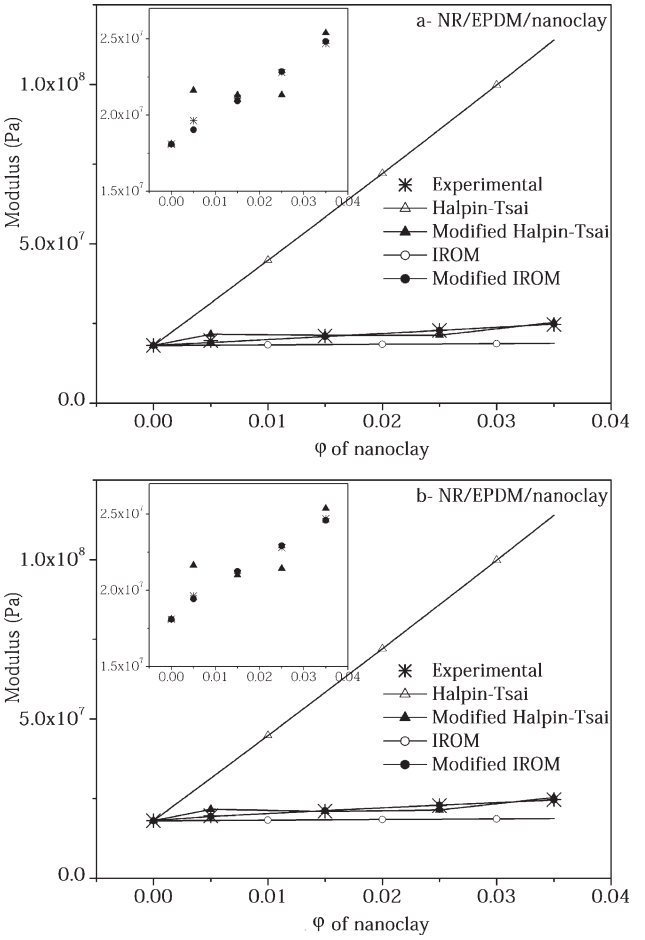

Figure 7. (a) Prediction of the Young's modulus of dispersed NR/EPDM/nanoclay composites for various amount of the nanoclay with modifying factor (I). (b) Prediction of the Young's modulus of dispersed NR/EPDM/nanoclay composites for various amount of the nanoclay with modifying factor (II).[28]

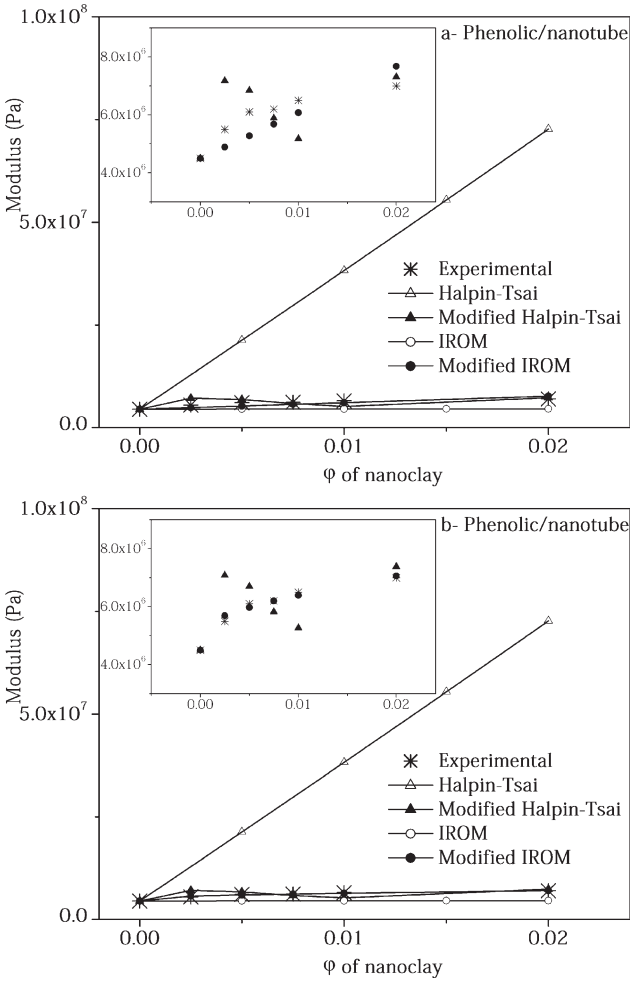

Figure 8. (a) Prediction of the Young's modulus of dispersed Phenolic/nanotube composites for various amount of the nanotube with modifying factor (I). (b) Prediction of the Young's modulus of dispersed Phenolic/nanotube composites for various amount of the nanotube with modifying factor (II).[5]

A comparative study of mechanical properties of PVC/NBR nanocomposite is carried out between the present experimental data and the prediction of theoretical models. The present analytical predictions are made for characteristic values of two kinds of nano-filler given in the "Experimental" section. Figure 4 shows the experimental Young's modulus and theoretical values against vol % of nano-filler obtained through LROM, IROM, and Halpin–Tsai models. The experimental and theoretical mechanical properties of PVC/NBR nanocomposites are listed in Table VII. As can be seen from Figure 4, the models IROM and Halpin–Tsai have rather better prediction in comparison with LROM. It is worth to note that there is still a significant variation in Young's modulus observed for both types of the mentioned models. Therefore, to cover Young's modulus of PVC/NBR nanocomposites in whole range of vol % of nano-filler, two modified form of both models can be expressed as:

$$E_{c(\text{Modified model})} = E_{\text{model}} \times \text{Modifying factor} \quad (21)$$

Where

$$\text{Modifying factor} = a\varphi_f + e^{b\lambda_L\varphi_f} e^{c\lambda_T\varphi_f} \quad \text{(I)}$$

$$\text{Modifying factor} = \varphi_f{}^a + e^{b\lambda_L\varphi_f} e^{c\lambda_T\varphi_f} \quad \text{(II)}$$

The proposed models are based on the modifying linear, exponential and power-law equations including orientation shape factor and volume concentration of nano-filler added into the original prediction equation. The modified models are rather sophisticated and there are three constant coefficients in the equation that must be properly determined to make a good prediction. These three parameters be determined experimentally via curve fitting procedure on the data of tensile test are given in Table VIII.

Before any inferences the accuracy of modified models should be checked. To This end, Figures 5 and 6 depict the predicted curve of Young's modulus versus vol % of nano-filler and the squared error of obtained modification values are given Table VII.

Table IX. Young's Modulus of Some Polymer Nanocomposites Predicted by Different Mechanical Models and Proposed Modified Models for Different Amounts of Nanofiller

		Analytical predictions for different specimens					
Sample	Experimental data[13,28]	Halpin-Tsai	IROM	(1) Modified Halpin-Tsai	(1) Modified IROM	(2) Modified Halpin-Tsai	(2) Modified IROM
NR/EPDM 0 vol % nanoclay	18.1e6	18.1e6	18.1e6	18.1e6	18.1e6	18.1e6	18.1e6
NR/EPDM 0.5 vol % nanoclay	19.6e6	31.3e6	18.2e6	20.1e6	19.0e6	21.6e6	19.4e6
NR/EPDM 1.5 vol % nanoclay	21.1e6	58.3e6	18.3e6	21.3e6	20.9e6	21.1e6	21.2e6
NR/EPDM 2.5 vol % nanoclay	22.8e6	86.4e6	18.5e6	22.3e6	22.8e6	22.4e6	22.9e6
NR/EPDM 3.5 vol % nanoclay	24.7e6	113.9e6	18.7e6	25.3e6	24.8e6	25.3e6	24.6e6
Phenolic 0 vol % nanotube	4.5e6	4.5e6	4.5e6	4.5e6	4.5e6	4.5e6	4.5e6
Phenolic 0.25 vol % nanotube	5.5e6	12.9e6	4.51e6	6.9e6	5.2e6	6.9e6	5.6e6
Phenolic 0.5 vol % nanotube	6.1e6	21.3e6	4.52e6	6.8e6	5.6e6	6.6e6	6e6
Phenolic 0.75 vol % nanotube	6.2e6	29.7e6	4.53e6	5.9e6	5.9e6	5.8e6	6.2e6
Phenolic 1 vol % nanotube	6.5e6	38.2e6	4.55e6	6.2e6	6.3e6	5.3e6	6.4e6
Phenolic 2 vol % nanotube	7e6	72.7e6	4.6e6	7.3e6	7.7e6	7.3e6	7e6

Table X. Parameters of Some Polymer Nanocomposites for Proposed Modifying Factor of IROM and Halpin–Tsai Models

Sample	Parameters of modifying factor	Nanoclay-filled NR/EPDM	Nanotube-filled Phenolic
(1) Modified Halpin-Tsai	**a**	4.719	4.629
	b	−0.237	−0.124
	c	6.673	3.634
(1) Modified IROM	**a**	9.239	33.627
	b	−0.034	−0.005
	c	6.962	5.023
(2) Modified Halpin-Tsai	**a**	0.498	0.598
	b	−0.273	−0.133
	c	6.713	3.794
(2) Modified IROM	**a**	0.582	0.235
	b	0.017	−.002
	c	−1.220	5.372

In order to further verify the accuracy of the proposed form of the models, comparisons were made using the experimental data reported by Alipour et al.[28] and Yeh et al.[5] for the Young's modulus of NR/EPDM/nanoclay and Phenolic/nanotube composites. It can be deduced from Figures 7 and 8(a,b) that our modification and predictions are almost coincident with Alipour and Yeh's results (for modeling purpose the density of nanoclay and nanotube assumed equal to 2 g/cm^3). The accuracy of the predicted Young's modulus is evident in Table IX. Small differences between the experimental data and predicted one show the good agreement of modified equations with the values of Young's modulus obtained from tensile tests. The parameters of fitting are given in Table X. Furthermore, provide enough information attributed to appropriate distribution of nanofiller in polymer matrix.[5,28]

CONCLUSION

Cloisite 30B, was used to reinforce the PVC/NBR matrix with various vol % of nanoclay. Good dispersion of nanofiller in PVC/NBR composites is proved by morphological investigations. The mechanical properties of PVC/NBR nanocomposites were measured by conducting tensile test. The addition of a few vol % of nanofiller exhibited a considerable increase in the Young's modulus and the tensile strength of the composite. It was shown that nanofiller content have a great impact on the degree of agreement between experimental data and theoretical data predicted by hyperelastic models. It should be noted that in the case of nanoclay-filled nanocomposites only second order Polynomial and Marlow can predict accurate behavior of strain-stress behavior. It was concluded that the nano-filler geometry can affect the tensile behavior of polymer matrix so that to investigate a modified models for prediction of nanocomposites is essential. Since the previous mechanical composite models reported in the literature such as LROM, IROM, and Halpin–Tsai were limited in their prediction to PVC/NBR nanocomposites; two more comprehensive predicting models were proposed on the basis of IROM and Halpin–Tsai. The presented modified models were identified by testing PVC/NBR nanocomposite specimens having various amounts of nanofiller. The modified form of models can not capable of replicating exactly the behavior of PVC/NBR nanocomposites, but it will give a reasonable approximation. Finally, a set of comparative studies with some available experimental data in the literature were performed to demonstrate the accuracy of the proposed models.

REFERENCES

1. Ismail, H.;Yusof, A. *Polym. Test.* **2004**, *23*, 675.
2. Hafezi, M.; Khorasani, S. N.; Ziaei, F. *J. Appl. Polym. Sci.* **2006**, *102*, 5358.
3. Coleman, J. N.; Khan, U.; Blau, W. J.l Gun'ko, Y. K. *Carbon* **2006**, *44*, 1624.
4. Pavlidou, S.; Papaspyrides, C. *Prog. Polym. Sci,* **2008**, *33*, 1119.
5. Yeh, M. K.; Tai, N. H.; Liu, J. H. *Carbon* **2006**, *44*, 1.
6. Wu, Y. P.; Jia, Q. X.; Yu, D. S.; Zhang, L. Q. *Polym. Test.* **2004**, *23*, 903.
7. Valavala, P.; Odegard, G. *Rev. Adv. Mater. Sci.* **2005**, *9*, 34.
8. Bokobza, L. *Polymer* **2007**, *48*, 4907.
9. Praveen, S.; Chattopadhyay, P. K.; Albert, P.; Dalvi, V. G.; Chakraborty, B. C.; Chattopadhyay, S. *Compos. Part A. Appl. Sci.* **2009**, *40*, 309.
10. Odegard, G. M.; Gates, T.; Wise, K. E.; Park, C.; Siochi, E. *Compos. Sci. Technol,* **2003**, *63*, 1671.
11. Fornes, T.; Paul, D. *Polymer* **2003**, *44*, 4993.
12. Clifford, M. J.; Wan, T. *Polymer* **2010**, *51*, 535.
13. Yeh, M. K.; Tai, N. H.; Lin, Y. J. *Compos. Part A. Appl. Sci.* **2008**, *39*, 677.
14. Kalaitzidou, K.; Fukushima, H.; Miyagawa, H.; Drzal, L. T. *Polym. Eng. Sci.* **2007**, *47*, 1796.
15. Bai, J. B. *Carbon* **2003**, *41*, 1325.
16. Omidi, M.; Rokni DT, H.; Milani, A. S.; Seethaler, R. J.; Arasteh, R. *Carbon* **2010**, *48*, 3218.
17. Affdl, J.; Kardos, J. *Polym. Eng. Sci.* **1976**, *16*, 344.
18. Liu, T.; Kumar, S. *Nano Lett.* **2003**, *3*, 647–650.
19. Esmizadeh, E.; Naderi, G.; Ghoreishy, M. H. R.; Bakhshandeh, G. R. *J. Polym. Eng.* **2011**, *31*, 83.
20. Esmizadeh, E.; Naderi, G.; Ghoreishy, M.; Bakhshandeh, G. *Sci. Technol. Polym.* **2010**, *23*, 293.
21. Brune, D. A.; Bicerano, J. *Polymer* **2002**, *43*, 369.
22. Hajibaba, A.; Naderi, G.; Esmizadeh, E.; Ghoreishy, M. H. R. *J. Compos. Mater.* **2012**;, DOI: 10.1177/0021998312469242.

23. Arasteh, R.; Omidi, M.; Rousta, A.; Kazerooni, H. *J. Macromol. Sci. Phys.* **2011**, *50*, 2464.
24. Termonia, Y. *Polymer* **2007**, *48*, 6948.
25. Rafiee, M. A.; Rafiee, J.; Wang, Z.; Song, H.; Yu, Z.-Z.; Koratkar, N. *ACS Nano* **2009**, *3*, 3884.
26. Gojny, F.; Wichmann, M.; Köpke, U.; Fiedler, B.; Schulte, K. *Compos. Sci. Technol.* **2004**, *64*, 2363.
27. Ali, A.; Hosseini, M.; Sahari, B. *J. Sci. Ind. Res. India* **2010**, *69*, 495.
28. Alipour, A.; Naderi, G.; Ghoreishy, M. H. R. *J. Appl. Polym. Sci.* **2012**, *127*, 1275.
29. Ghasemi, I.; Karrabi, M.; Ghorieshy, M. *Plast. Rubber. Compos.* **2008**, *37*, 305.
30. Barkoula, N. M.; Karger-Kocsis, J. *Wear* **2002**, *252*, 80.
31. Jalham, I. S.; Maita, I. J. *J. Compos. Mater.* **2006**, *40*, 2099.
32. Cataldo, F. *Macromol. Symp.* **2007**, *247*, 67.
33. Mazurkiewicz, D. *Arch. Civil. Mech. Eng.* **2009**, *9*, 75.
34. Austrell, P. E.; Kari, L. In Constitutive Models for Rubber IV: Proceedings of the Fourth European Conference on Constitutive Models for Rubber, Stockholm, Sweden, June 27–29, **2005**.
35. Dorfmann, A.; Muhr, A. In Constitutive Models for Rubber: Proceedings of the First European Conference on Constitutive Models for Rubber, Vienna, Austria, September 9–10, **1999**.
36. Duncan, B. C.; Crocker, L. E.; Urquhart, J. M. Evaluation of Hyperelastic Finite Element Models for Flexible Adhesive Joints, National Physical Laboratory, **2000**.
37. Korochkina, T.; Claypole, T.; Gethin, D. In Constitutive Models for Rubber IV: Proceedings of the Fourth European Conference on Constitutive Models for Rubber, Stockholm, Sweden, June 27–29, **2005**.
38. Ghosh, P.; Saha, A.; Mukhopadhyay, R. Constitutive Models for Rubber III: Proceedings of the Third European Conference on Constitutive Models for Rubber, London, UK, September 15–17, **2003**.
39. Esmizadeh, E.; Naderi, G.; Ghoreishy, M. H. R.; Bakhshandeh, G. R. *Iran. Polym. J.* **2011**, *20*, 587.
40. Lu, L.; Zhai, Y.; Zhang, Y.; Ong, C.; Guo, S. *Appl. Surf. Sci.* **2008**, *255*, 2162.
41. Mousa, A.; Halim, N.; Al-Robaidi, A. *Polym. Plast. Technol.* **2006**, *45*, 513.
42. Alipour, A.; Naderi, G.; Bakhshandeh, G.; Vali, H.; Shokoohi, S. *Int. Polym. Proc.* **2011**, *26*, 48.
43. Allaoui, A.; Bai, S.; Cheng, H. M.; Bai, J. *Compos. Sci. Technol.* **2002**, *62*, 1993.
44. Galgali, G.; Agarwal, S.; Lele, A. *Polymer* **2004**, *45*, 6059.